

PAPER • OPEN ACCESS

Role of infernal modes dynamics and plasma rotation on the onset of NTMs in ECH-ECCD TCV plasmas

To cite this article: D Brunetti *et al* 2016 *J. Phys.: Conf. Ser.* **775** 012002

View the [article online](#) for updates and enhancements.

Related content

- [Nonlinear mode coupling during NTMs](#)
D Raju, O Sauter and J B Lister
- [Long timescale density peaking in JET](#)
M Valovic, J Rapp, J G Cordey et al.
- [Extended MHD simulations of infernal mode dynamics and coupling to tearing modes](#)
D Brunetti, J P Graves, F D Halpern et al.

Recent citations

- [Physics conditions for robust control of tearing modes in a rotating tokamak plasma](#)
E Lazzaro *et al*



IOP | ebooks™

Bringing you innovative digital publishing with leading voices to create your essential collection of books in STEM research.

Start exploring the collection - download the first chapter of every title for free.

Role of infernal modes dynamics and plasma rotation on the onset of NTMs in ECH-ECCD TCV plasmas

D Brunetti, E Lazzaro, S Nowak

Istituto di Fisica del Plasma IFP-CNR, Via R. Cozzi 53, 20125 Milano, Italy

O Sauter, J P Graves

*École Polytechnique Fédérale de Lausanne (EPFL), Swiss Plasma Center (SPC),
CH-1015 Lausanne, Switzerland*

E-mail: brunetti@ifp.cnr.it

Abstract. Experiments in the TCV tokamak show that when high power central electron cyclotron heating (ECH) and current drive (ECCD) are deposited in the central plasma region, tearing-like instabilities can develop. In the present work we address, both analytically and numerically, the problem of tearing mode (TM) generation analysing extensively the behaviour of L-mode and low plasma current TCV discharges when high power heating is deposited in the plasma core region. Three possible mechanisms are discussed. The first is the modification of the equilibrium current density profile due to the power deposition leading to variation of the sign of the classical tearing stability index Δ' , where finite β effects could also be taken into account. The second mechanism still the modification of the tearing stability parameter Δ' , but this time due to the presence of an equilibrium sheared toroidal plasma rotation. Finally, the third mechanism considered is the role of *infernal-type* instabilities in driving tearing-like modes when the safety factor becomes sufficiently close to a rational in the core region.

1. Introduction

One of major issues in present day tokamak theory, is to understand the mechanisms which cause the onset of dangerous tearing-like instabilities. In absence of the standard tearing drive (i.e. current density gradient), neoclassical tearing modes (NTMs) can be driven unstable if "seeded" by other sources of magnetic perturbations, such as e.g. sawteeth and ELMs. In absence of these triggers, the onset of NTMs is still unexplained and it must be carefully investigated on the basis of the experimental evidence. Experimental observations in L-mode and low plasma current TCV discharges, showed the presence suddenly growing NTMs when high power heating is deposited in the plasma core region. This occurred without usual triggers such as sawteeth or ELMs [2] although a small 1/1 MHD activity was detected.

Hence this work we address the problem of NTM generation analysing a realistic TCV configuration when central power deposition and electron current drive (ECCD) are applied. We can think of three possible mechanisms for the triggering of these sudden tearing modes:

- a positive and possibly very large Δ' ($\Delta' = \psi'/\psi|_{r_s+\epsilon}^{r_s-\epsilon}$ [1]) due to the equilibrium current density profile modification
- a Δ' modification due to the effect of the equilibrium toroidal rotation



- a coupling between harmonics induced by the loss of field line bending in the core due to the flatness of the safety factor (infernial mechanism)

As proposed in Ref. [2], one of the driving mechanisms for the onset of these instabilities can be the modification of the equilibrium current density profile with a variation of the sign of the classical tearing stability index Δ' . Modifications of Δ' can be due also to finite β effect [3]. Indeed ECH and ECCD alter both the profile of the pressure, which is increased, and of the current viz. the safety factor which could be modified both at the position of q -rational surface of the observed NTM. These two effects combined could produce a change in Δ' leading to an effective classically unstable tearing mode. Modification of Δ' are also expected when the intrinsic equilibrium plasma rotation is taken into account [4].

From the equilibrium reconstruction and from the fact that there is a very small 1/1 MHD activity the safety factor appears to be shear-free over a fairly broad region in the core (up to $\rho_\psi \sim 0.35$) with $q \geq 1$. Configurations in which magnetic shear is allowed to become small over a large region, *infernial modes* can be driven unstable by the core pressure gradients if the core safety factor is sufficiently close to a rational number [5]. Infernial modes are characterised by toroidicity induced coupling between a core mode (with wave number (m, n)) and its neighbouring resistive sidebands (with wave number $(m \pm 1, n)$) which can grow on very fast timescales [6, 7] without the presence of usual triggers (e.g. sawteeth, ELMs). In particular we might expect co-current ECCD deposition should lower the central safety factor so that conditions for *infernial instability* are met. Hence infernial modes can be considered to be possible candidate to explain the onset of TMs observed experimentally.

Summarising, various mechanisms for the NTM generation are analysed having as a reference point a realistic TCV configuration with central ECH and ECCD. In section 2 we discuss the impact of the equilibrium sheared toroidal plasma rotation on Δ' assessing quantitatively its total modification with parameters typical for machines such as TCV, NSTX and DIII-D. Section 3 focuses on the numerical estimate of the classical Δ' (no rotation, classical TM). First we describe a novel code for the calculation of Δ' , capable of handling realistic complex geometries without approximations on the metric elements. Then a series of four TCV discharges is analysed where the numerical computation of the tearing stability index is performed. Finally section 4 presents a parametric study of the resistive infernial stability in such configurations providing an estimate of the ideal threshold for these modes. Finally we summarise in section 5.

2. Sheared rotation effects on Δ'

It is known that plasma rotation can have a significant effect on the nonlinear behaviour of a tearing mode [8]. But how big is the impact of the flow on the linear stability of a TM? The aim of this section is thus to investigate analytically the effects of toroidal plasma rotation on Δ' .

We set ourselves in a cylindrical coordinate system (r, ϑ, φ) where the magnetic field is given by

$$\mathbf{B} = \nabla F \times \nabla \vartheta - \nabla \psi \times \nabla \varphi. \quad (1)$$

The contravariant and covariant components of a vector \mathbf{A} are given by $A^i = \mathbf{A} \cdot \nabla q^i$ and $A_i = \mathbf{A} \cdot \mathbf{e}_{q^i}$, where ∇q^i and \mathbf{e}_{q^i} are the contravariant and covariant basis vectors respectively. We assume constant (both in space and time) mass density and the toroidal magnetic field. The equilibrium velocity is imposed to be $\mathbf{v}_0 = \Omega(r)\hat{\mathbf{e}}_\varphi$. In order to simplify the analysis we choose a reference frame which is moving along the axis of the cylinder such that $\Omega(r_s) = 0$ [9]. Let Ω_0 be the rotation frequency on the magnetic axis.

Multiplying the force balance equation by $1/B^\varphi$ and then taking the $\nabla \varphi$ projection of its curl, leads to (for sake of simplicity we set $\Omega \equiv \Omega(r)$):

$$\frac{\rho}{B^\varphi} \nabla \varphi \cdot \nabla \times (\mathbf{v} \cdot \nabla \mathbf{v}) = \mathbf{B} \cdot \nabla \left(\frac{J^\varphi}{B^\varphi} \right), \quad (2)$$

where finite β effects have been neglected.

A very simple Newcomb-like differential equation for the radial fluid displacement X is obtained by linearising (2) and the Faraday-Ohm's law with a parabolically distributed current [10]:

$$\frac{d}{dz} \left[z^2 [(1-z)^2 - \hat{\Omega}^2] \frac{dX}{dz} \right] + \left\{ \frac{(1-m^2)}{\lambda^2} [(1-z)^2 - \hat{\Omega}^2] - 2z \frac{\hat{\Omega}}{\lambda^2} \frac{d\hat{\Omega}}{dz} \right\} X = 0,$$

where the normalised variable $z = (r/r_s)^2$ has been introduced. The detailed analytic derivation is beyond the scope of this paper and it will be reported in a future publication. We limit ourselves to present the main results. For a parabolically distributed current density and toroidal rotation, the tearing stability parameter Δ' is found to be (see e.g. Ref. [10]):

$$r_s \Delta' = \frac{\bar{m}^2 - m^2}{2} \pi \cot \pi \xi, \quad (3)$$

where $\xi = \frac{m-\bar{m}}{2}$ and $\bar{m} = \sqrt{m^2 + 8 + 4U}$. We defined the parameter $U = \frac{2[\Omega_0/(\hat{s}\omega_A)]^2}{1-[2\Omega_0/(\hat{s}\omega_A)]^2}$, where $\omega_A = B_0/(\sqrt{\rho_0}R)$ is the Alfvén frequency and $\hat{s} = r_s q'_s/q_s$.

Assuming a magnetic shear of order of unity and $\Omega_0/\omega_A \sim 10^{-2} \div 10^{-3}$ [2, 8, 11], then Δ' is approximated by its usual cylindrical value plus a small correction which is found to be positive in agreement with Ref. [4], viz.:

$$r_s \Delta' \approx r_s \Delta'_{cyl} + \delta,$$

with $0 < \delta \ll 1$. We therefore conclude that rotation effects on the modification of the equilibrium Δ' are negligible.

3. Δ' estimate in ECH-ECCD TCV discharges

Before analysing the experimental TCV discharges, we describe the numerical code employed for the calculation of the stability index Δ' . This code works in a standard MHD frame where no equilibrium flows are considered, allowing in principle for finite β effects. Finite β corrections however are not taken into account in the analysis performed. We point out that in a realistic tokamak configuration shaping effects are not negligible. This is seen e.g. on the value of the edge safety factor in which the theoretical cylindrical model can differ up to the 30% wrt the real experimental value. Thus we developed our code in order to handle a generic tokamak geometry without any approximation.

The perturbed poloidal flux is calculated in a straight field line coordinate system (r, ϑ, φ) where the magnetic field is given by (1) and the radial variable r is normalised such that $r = 1$ at the plasma boundary. The radial variable can be defined in terms of either the poloidal flux ($r \sim \sqrt{\frac{\psi - \psi_0}{\psi_{edge} - \psi_0}}$) or the toroidal flux ($r \sim \sqrt{\frac{F - F_0}{F_{edge} - F_0}}$) where ψ and F are as in (1) and the subscript 0 indicates that the quantity is evaluated on the magnetic axis. There is not a significant difference in the final results between the two definitions. Hence we decided to work with r defined in terms of the poloidal flux. In this coordinate system \sqrt{g} denotes the Jacobian and $g_{i,j}$ ($i, j = r, \vartheta, \varphi$) are the elements of the metric tensor.

Multiplying the force balance equation by $1/B^\varphi$ and then taking the $\nabla\varphi$ projection of its curl, after linearisation we have for the m th Fourier component of the perturbed flux (0 indicates equilibrium quantities):

$$\psi_m'' = A_1 \psi_m' + \left(A_2 + \frac{A_3}{m\mu - n} \right) \psi_m, \quad (4)$$

where the Faraday-Ohm's law has been used, $\mu = 1/q$, $J_* = J_0^\varphi/B_0^\varphi$, and the coefficients A_i ($i = 1, 2, 3, 4$) are given by:

$$A_1 = -\langle g_{\vartheta\vartheta}/\sqrt{g} \rangle^{-1} \langle g_{\vartheta\vartheta}/\sqrt{g} \rangle', \quad A_2 = m^2 \langle g_{\vartheta\vartheta}/\sqrt{g} \rangle^{-1} \langle g_{rr}/\sqrt{g} \rangle, \quad A_3 = m \langle g_{\vartheta\vartheta}/\sqrt{g} \rangle^{-1} \langle J_* \rangle',$$

with $\langle A \rangle = \frac{1}{2\pi} \int_0^{2\pi} A d\vartheta$. In deriving the expression above we used the fact that $\langle g_{r\vartheta}/\sqrt{g} \rangle = \langle g_{r\vartheta}/\sqrt{g} \rangle' \sim 0$ and we neglected perturbations of the toroidal field. Note that no assumptions were made on the geometry of the system apart from the imposition of the vanishing average of the off diagonal elements of the metric tensor. We impose boundary conditions $\psi_m(0) = \psi_m(1) = 0$.

The code reads an OUTXOR-CHEASE equilibrium [12], viz. pressure and current profiles and the shaping of the magnetic surfaces. The CHEASE equilibrium needs as input plasma pressure and the toroidal current I^* giving as output the safety factor, required for the stability calculation. A recent update of the code [13] allows to provide as input the safety factor. This new feature is not used in the preset work but it will be useful in further studies for a simpler and more rapid estimate of Δ' .

First the straight field line poloidal angle is calculated (see e.g. [14]). The metric tensor elements $g_{i,j}$ and their averages are calculated by Fourier decomposing the magnetic surfaces in ϑ . In this manner the calculation of the radial and poloidal derivatives (of e.g. the toroidal current) becomes straightforward. Once we have all the physical quantities, the coefficients A_i ($i = 1, 4$) can be evaluated.

We note that for $m = 2$ the evaluation of Eq. (4) becomes problematic since the coefficient A_1 is singular on the magnetic axis while $\psi_m'' \neq 0$ (this is clear because near the magnetic axis the perturbed poloidal flux is expected to behave as $\psi_m \sim r^m$). Hence when $m = 2$, equation (4) is solved in the region $0 < r < r_s$ with a RK4 method with the following initial conditions at r_0 near the magnetic axis (Cauchy problem):

$$\psi_m \sim r_0^m, \quad \psi_m' \sim m r_0^{m-1} \quad (5)$$

When $m \geq 3$ we have that $\psi_m'' = 0$ on the magnetic axis so that the shooting method implemented with an RK4 procedure can be employed in which we "shoot" the solution either from the magnetic axis to the resonant point or the other way around. The shooting method (away from r_s to the plasma boundary) is used in the region $r_s < r < 1$ for any m since in this region the coefficients A_i are well defined. We note that instead of using a shooting procedure for solving ψ_m when $m \geq 3$ in the region $0 < r < r_s$, we can define an analogous Cauchy problem as already done for the $m = 2$ case (cf. Eq. 5). The final result is practically identical to the one obtained with the shooting method, hence in our calculation we always (i.e. for any m) assume a Cauchy problem of the type (5) in the region $0 < r < r_s$. In order to increase the accuracy of the evaluation of the tearing eigenfunction the radial mesh becomes finer as the resonant surface of the mode is approached.

Finally, ψ_m' is fitted with a logarithmic least square fitting algorithm with a function of the type $\psi_m' \sim a_L + b_L \ln(x)$ for $x < 0$ and $\psi_m' \sim a_R + b_R \ln(x)$ for $x > 0$, where $x = r - r_s$ and $\Delta' = a_R - a_L$.

Excellent agreement is found in the large aspect ratio limit with the theoretical results given in Ref. [3]. As a preliminary result, we have also implemented finite β effects. When β effects are switched off Δ' reduces to the zero pressure case. In addition, in line with Ref. [15], we checked that $\Delta' \rightarrow -2$ as $D_I \rightarrow \frac{1}{4}$ (i.e. pressure increased), which guarantees the well behaviour of the algorithm. However since a more refined modelling of the finite pressure effects is required, β corrections will not be considered when we discuss the application of the code for the analysis of realistic TCV discharges. This will be presented in the next section.

3.1. Analysis of TCV discharges #488(36),(37),(39),(41)

We analyse four TCV shots, namely #488(36),(37),(39),(41). The two key parameters of interest for our study are the pressure profile and the shape of the safety factor, i.e. the plasma current density. These two quantities are modified during time both due to central ECH and ECCD.

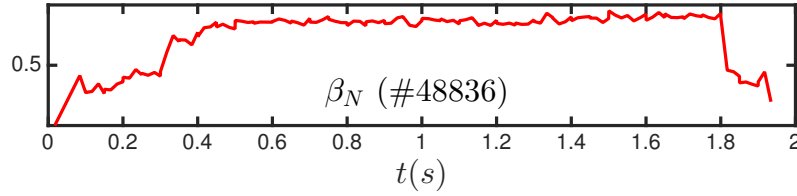


Figure 1. Time evolution of β_N for shot #48836. A similar behaviour is also observed for shots #488(37),(39),(41). The time trace of the profile remains qualitatively and quantitatively similar, despite MHD activity is present (cf. Fig. 2).

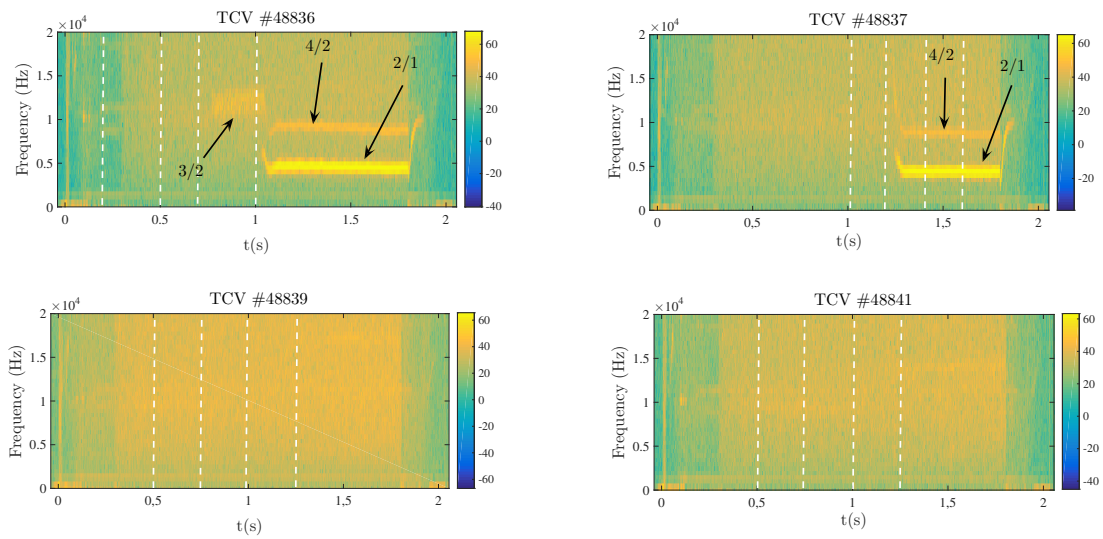


Figure 2. Spectrograms of TCV discharges #488(36),(37),(39),(41). No MHD activity is recorded in shots #488(39),(41), where the current injection was counter-current. Shots #488(36),(37) with co-current injection show a low m MHD activity: modes 3/2 and 2/1 are observed in shot #48836 while only the 2/1 is observed in shot #48837. The dashed white vertical lines correspond to the times at which the safety factor profiles shown in figure 3 are taken.

The current injection is mainly in the co- I_P (I_P is the plasma current) direction for discharges #488(36),(37) and mainly in counter- I_P direction for shots #488(39),(41). The ECH phase starts in the four discharges at $t \sim 0.2 - 0.3$ s. This causes a sudden rise of the pressure as it is clearly visible in the time trace of the evolution of $\beta_N (= \beta a B_T / I_P$, where a is the minor radius and B_T is the toroidal magnetic field on the axis) shown in Fig. 1. No significant variations in β_N are observed as the 3/2 and 2/1 TMs appear. Figure 2 shows the spectrograms for the four discharges analysed. We see that MHD activity is present in shots #488(36),(37) (co- I_P ECCD) while discharges in #488(39),(41) no TM activity is reported.

In order to evaluate Δ' , we need a CHEASE equilibrium which is obtained from the instantaneous equilibrium reconstruction via the LIUQE code [16]. Once the CHEASE equilibrium is calculated we are able to compute numerically the instantaneous tearing stability index Δ' with the code described in the previous section.

The safety factor profiles taken at the times indicated in Fig. 2 are shown in figure 3. First

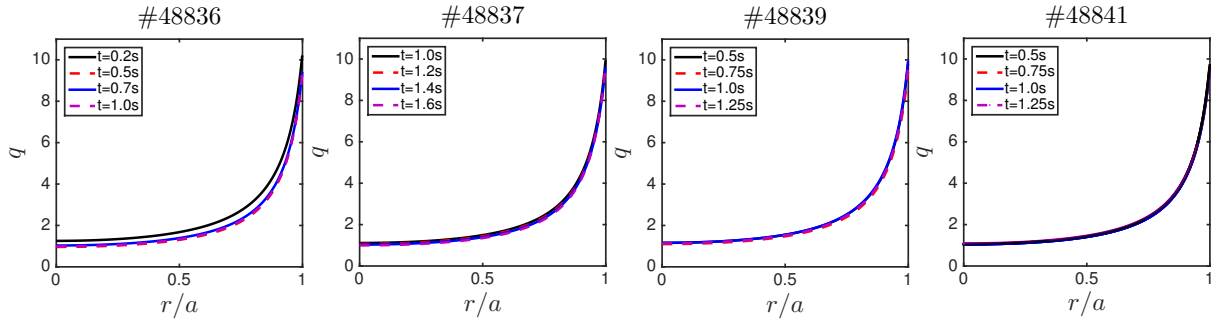


Figure 3. Radial safety factor profiles taken at different times for the shots of the series #488(XX) considered. Note that there are no dramatic variations at the 2/1 and 3/2 resonant surfaces.

of all we note that the MHD activity does not appear immediately after the ECH and ECCD deposition. This might suggest that the mechanism of the onset of the TMs observed should be contained in the variations of the current density profile. From figure 3, we note that in the four shots the variations q during time after the ECH deposition phase are not dramatic (e.g. at the 2/1 resonant surface). We however may expect substantial differences in q'' , leading to different values of the stability parameter Δ' . Hence we can numerically calculate Δ' for the Fourier modes 2/1, 3/2, 3/1, 4/2 and 4/3. This is shown in figure 4 where finite β effects have been dropped. It is observed that when $\beta = 0$, the 2/1 mode has always a positive Δ' , contrarily to what we expect from the experimental observation for shots #488(39),(41) where this mode is stable which would imply $\Delta' < 0$. In addition we note that in shots #488(36),(37) Δ' of the mode 2/1 is found to be positive well before the onset of the instability. This could be an indication that a more subtle underlying physics has to be considered. It is however found that modes with $m \geq 3$ are stable ($\Delta' < 0$) in all four shots so that the mechanism of a simple modification of the current profile (i.e. q) at the mode resonant surface is not sufficient for explaining the onset of the 3/2 mode observed in discharge #48836. In the next section we discuss the third mechanism which could explain this behaviour.

4. Role of the infernal mode mechanism for the TM onset

As shown in figure 1, in all four shots β_N does not have significant variations when the resistive modes appear. In particular the four discharges analysed have almost the same pressure profile. Thus we might expect to be unlikely that the MHD activity reported depends solely on the rise of the pressure due to the ECH. As shown in figure 5, the CHEASE reconstructed q profile is very close to $q = 1$ over a rather large region which extends from the magnetic axis to $r/a \sim 0.3$. We recall that shots #488(36),(37) were performed globally in co- I_p ECCD (3 gyrotrons in co- I_p for #48836 and 2 gyrotrons in co- I_p and 1 in counter- I_p for #48837) with a consequent increase of the total I_P . Conversely shots #488(39),(41) were globally in counter- I_p ECCD (2 gyrotrons in counter- I_p and 1 in co- I_p in #48839 and 1 gyrotron in counter- I_p , 1 in co- I_p and 1 gytron in heating in #48841) with a decrease of I_p . It is known that an increase of the total current leads to a small decrease of q , i.e. the safety factor is shifted downwards almost rigidly [17]. On the other hand a decrease of the total current should "lift" the q .

This might suggest that an infernal-like mechanism could occur in which a core 1/1 (2/2) mode couples with its 2/1 (3/2) tearing sideband. In particular small 1/1 activity was measured in shot #48836 although invisible on the spectrograms in figure 2 (this could be due to the fact that these are internal modes with a not too large amplitude). Infernal modes are more

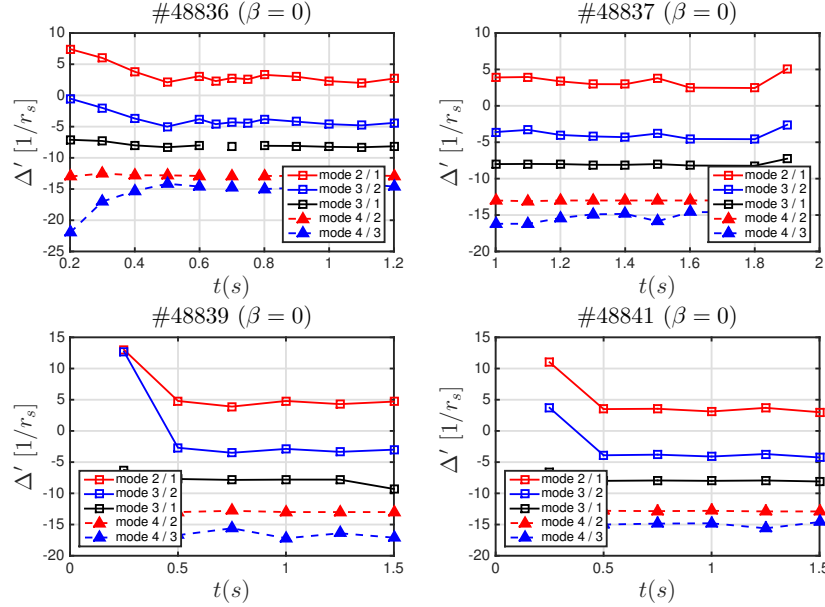


Figure 4. Values of Δ' computed numerically for discharges #488(36),(37),(39),(41) where the modes 2/1,3/2,3/1,4/2 and 4/3 are considered under the assumption $\beta = 0$. Although no MHD signals were observed in shots #488(39),(41) as shown in Fig. 2, the code still gives a positive definite Δ' for the 2/1 mode which appears to contradict the experimental observation.

unstable if the core safety factor is close to the rational and are stabilised as q is pushed away. This could explain why in discharges #488(36),(37) MHD activity is observed while being absent in shots #488(39),(41). This mechanism thus appears to be plausible and not in contrast with the experimental observations. We focus our analysis on the 3/2 mode since the 2/1 mode was numerically found to be unstable requiring further study to find an agreement with experimental observations.

We know that if the tearing stability index is negative, a threshold for the onset of the resistive infernal mode in the value of q_{min} for a fixed β_p is expected [5]. This means that by writing $q = 1 + \delta q$ it does exist a critical value δq_{crit} so that if $\delta q < \delta q_{crit}$ the coupling occurs and the resistive sideband is unstable. If $\delta q > \delta q_{crit}$ the resistive sideband is stabilised. The same argument hold when we swap δq with β_p , i.e. we fix δq and let β_p to vary. Of course in this case the threshold is given by a critical value of poloidal β (i.e. $\beta_{p,crit}$) so that if $\beta_p > (<) \beta_{p,crit}$ the mode is unstable(stable). This in principle could explain the sudden appearance of the tearing instability as observed in Fig. 2.

Expressing the safety factor in the central region where it is almost flat as $q \approx 1 + \delta q$, the threshold is found by setting $\gamma = 0$ (γ is the growth rate) and gives the following equation for a fixed poloidal mode m :

$$\delta q = \sqrt{-\beta_{p,*}^2 G_0 \frac{M_0}{A_0}}, \quad (6)$$

where β_p is the poloidal β and it is evaluated at the transition radius r_* where the magnetic shear $\hat{s} = (rdq/dr)/q$ becomes smaller than unity, i.e. where $\hat{s}(r = r_*) \approx 1$ (all the quantities with the subscript $*$ are evaluated at the point $r = r_*$). We defined $\varepsilon = r/R_0$, $G_0 = \frac{\varepsilon_*^2 \hat{s}_* / (\hat{s}_* - 2)}{m(m+1)}$, A_0 and M_0 are a measure of the amplitude of the jump of the eigenfunction across the resonant surface

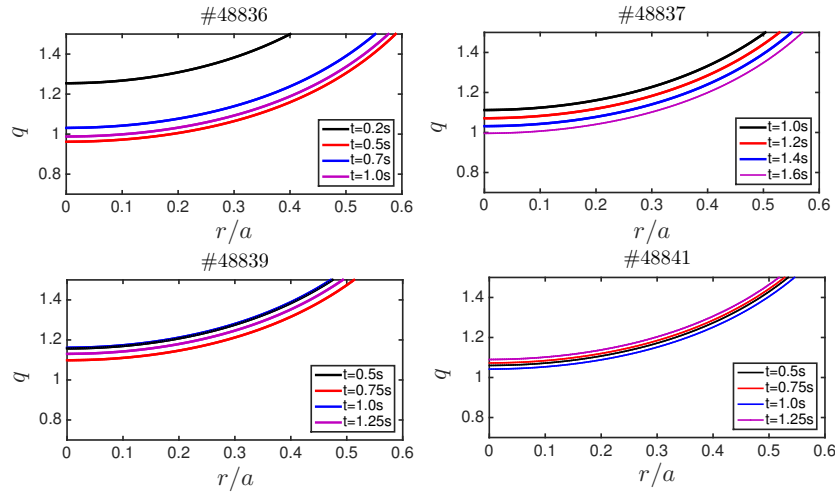


Figure 5. Radial safety factor profiles obtained from CHEASE equilibrium reconstruction taken at different times for the shots of the series #488(XX) considered (times taken as in Fig. 3). We note that for shots #488(36),(37) the central q is closer to unity compared with discharges #488(39),(41). This might suggest that an infernal-like mechanism is plausible for the triggering of the modes.

of the mode (A_0 is the standard tearing Δ' and M_0 is the jump of the second eigenfunction which is usually dropped because of the divergence on the magnetic axis).

Letting A_0 and M_0 vary (usually in the cylindrical limit $M_0 < 0$) and assuming a stable mode with $A_0 < 0$ we obtain the threshold value for δq_{crit} below which the mode becomes unstable. This is reported in Fig. 6, where we used the experimental values of TCV shot #48836 for β_P , ε and \hat{s} for the 3/2 mode for which $\Delta' < 0$ (cf. Fig. 4). In this case we have $r_*/a \approx 0.3$. We find $\delta q_{crit} \sim 0.1$ which is consistent with the shape of the safety factor shown in Fig. 5. Thus an infernal-like mechanism could be invoked as a valid candidate for the explanation of the onset of the 3/2 mode in TCV discharge #48836.

5. Conclusions

Three possible mechanisms for the explanation of the onset of TMs in realistic TCV discharges have been analysed. First the role of the equilibrium intrinsic toroidal rotation has been assessed. It is found that for realistic values of the toroidal rotation (valid for TCV, DII-D and NSTX tokamaks), the value of Δ' is only weakly increased leading us to rule out such effect as a possible trigger for the sudden appearance of TMs.

The second mechanism analysed is the modification of the safety factor profile, i.e. current density, due to the combined action of central ECH and ECCD deposition. A modification of the current density profiles leads to a variation of Δ' . In order to evaluate numerically Δ' , a novel code has been developed which allows an accurate determination of the tearing stability index without any approximation on the geometry. This code has been used to analyse four TCV discharges (#488(36),(37),(39),(41)). It has been found that modes with $m \geq 3$ are stable ($\Delta' < 0$) while the $m = 2$ always presents a positive Δ' . This cannot explain such a sharp rise of TMs and suggests that a more subtle physics has to be unravelled.

Finally the role of the infernal mechanism for the 3/2 mode has been assessed. It is found that in the range of parameters typical of the four TCV shots analysed, the threshold of the resistive mode is not too far from the experimental evidence. Moreover this mechanism appears to be

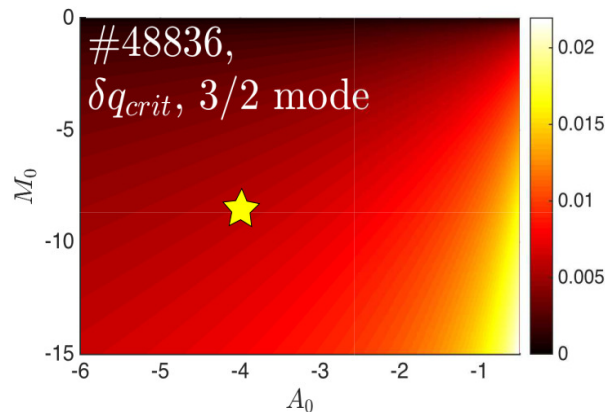


Figure 6. Threshold in δq for the mode 3/2 with the safety factor and β_p of the shot #48836. As the mode becomes more stable (decreasing A_0) δq_{crit} decreases. This means that instability window $\delta q < \delta q_{crit}$ for which the mode is unstable becomes narrower, i.e. q has to be very close to unity to drive and instability and if it lies outside this window no mode is expected. Experimental values of A_0, M_0 for shot #48836 are indicated by the star.

plausible and not in contrast with the experimental observations since resistive MHD activity was reported only in shots with co- I_P ECCD, i.e. when infernal unstable conditions are met.

Further future investigation will focus on a more refined description of the finite β effects and in particular analysing the nonlinear behaviour described by the generalised Rutherford equation taking into account possible variations in the sign of the polarisation term in the generalised Rutherford equation [2, 18]). It is envisaged that this work will guide the nonlinear work to follow.

Acknowledgments

This work, performed under the European Fusion Development Agreement, was supported by the European Communities, the Istituto di Fisica del Plasma CNR and the Swiss National Science Foundation. The views and opinions expressed herein do not necessarily reflect those of the European Commission.

References

- [1] Wesson J A 2011, **Tokamaks** (Oxford U. P., Oxford, UK)
- [2] Lazzaro E et al. 2015 *Nucl. Fusion* **55** 093031
- [3] Hegna C C and Callen J D 1994 *Phys. Plasmas* **1** 2308
- [4] Sen A, Chandra D and Kaw P 2013 *Nucl. Fusion* **53** 053006
- [5] Brunetti D, Graves J P, Cooper W A and Wahlberg C 2014, *Plasma Phys. Control. Fusion* **56** 075025
- [6] Charlton L A, Hastie R J and Hender TC 1989 *Phys. Fluids B* **1** 798
- [7] Brunetti D, Graves J P, Halpern F D, Luciani J-F, Lütjens H and Cooper W A 2015, *Plasma Phys. Control. Fusion* **57** 054002
- [8] La Haye R J, Brennan D P, Buttery R J and Gerhardt S P 2010 *Phys. Plasmas* **17** 056110
- [9] Chen X L and Morrison J P 1990 *Phys. Fluids B* **2** 495
- [10] Mikhailovskii A B 1998 *Instabilities in a Confined Plasma* (IOP, Bristol)
- [11] Wang F, Fu G Y, Breslau J A, Tritz K and Liu J Y 2013 *Phys. Plasmas* **20** 072506
- [12] Lütjens H, Bondeson A and Sauter O 1996 *Comput. Phys. Commun* **97** 219
- [13] Blondel L 2016 *Axisymmetric Tokamak Equilibria computed with a Predefined Safety Factor Profile as CHEASE input* (EPFL Master Project)
- [14] Hirshman S P and Whitson J C 1983 *Phys. Fluids* **26** 3553

- [15] Nishimura Y, Callen J D and Henga C C 1998 *Phys. Plasmas* **5** 4292
- [16] Moret J-M, Duval B P, Le H B, Coda S, Felici F and Reimerdes H 2015 *Fusion Eng. Des.* **91** 1
- [17] Cooper W A, Graves J P and O Sauter O 2011 *Plasma Phys. Control. Fusion* **53** 024002
- [18] Smolyakov A I, Hirose A, Lazzaro E, Re G B and Callen J D 1995 *Phys. Plasmas* **2** 1581